Communication

Low-Temperature Stability and High-Temperature Reactivity of Iron-Based Core–Shell Nanoparticles

Christopher E. Bunker, and John J. Karnes

J. Am. Chem. Soc., **2004**, 126 (35), 10852-10853• DOI: 10.1021/ja0473891 • Publication Date (Web): 17 August 2004

J|A|C|S
COMMUNICATIONS

Published on Web 08/17/2004

Low-Temperature Stability and High-Temperature Reactivity of Iron-Based Core−Shell Nanoparticles

Christopher E. Bunker* and John J. Karnes

Air Force Research Laboratory, Propulsion Directorate, Wright-Patterson AFB, Ohio 45433

Received May 4, 2004; E-mail: christopher.bunker@wpafb.af.mil

Engineering the surface of nanoparticles to tailor physical or chemical properties for desired effects is the focus of numerous research efforts. Interesting examples of core−shell nanoparticles with unique or enhanced optical, magnetic, and catalytic properties are well documented.[1−4] As the particle size decreases, the surface area increases, offering the promise of enhanced reactivity, greater efficiency, and potentially new and unusual active sites. A problem arises when the active sites of the nanomaterial are unstable under ambient conditions. Methods to protect the active material from early or undesired reactions are required if easy, cost-effective applications of these materials are to be realized. We have been investigating the development of such methods using Fe^0 nanoparticles as model compounds. These nanoparticles are easy to produce by the sonochemical method[5,6] and can be combined with a number of organic materials both in situ and after-the-fact to form core−shell nanoparticles.[7,8] In some cases, the core−shell nanoparticles are resistant to oxidation, which prevents the conversion of the Fe^0 core to an oxide form (Fe_xO_y). These observations agree well with results from other core−shell nanoparticle systems, specifically Co[9,10] and FePt[11] nanoparticles with various organic stabilizers, prepared using high-temperature reduction or decomposition methods. Here, we demonstrate the oxidative stability of two Fe-based core−shell materials and, more importantly, the ability to regain reactivity using temperature as a trigger.

In the preparation of the iron nanoparticles, a deoxygenated solution of $Fe(CO)_5$ in dodecane (0.11 M) was sonicated for 15 min active time using a 1 s on, 1 s off procedure. In the absence of the organic-shell component, the solution quickly turned dark, and solid material was observed to settle out of solution. Once recovered, the dark solid material (Fe^0 nanoparticles) easily converted to a reddish solid (Fe_xO_y) upon exposure to air or water. The same reaction performed with dioctyl sulfosuccinate sodium salt (AOT) or oleic acid present in solution at a concentration of 0.1 M produced a dark solution that yielded no precipitate. The solutions were stable for a time period on the order of months and showed no visible changes upon exposure to air or water. FTIR analysis of the core−shell nanoparticles indicated chemical bonding of the organic component to the iron-particle surface (Figures 1a and 1b).[7] TEM analysis revealed nanoparticles with an average size of ∼7 nm (Figure 1c and 1d) and an interesting ring pattern. Such patterns have been observed in TEM images of sonochemically produced bimetallic nanoparticles;[12] however, in those cases, the darker regions represent the cores. The particles shown in Figure 1c reveal a darker region on the outside of the particle. The reactivity of the Fe^0 nanoparticles was investigated using the reaction of oxygen with Fe^0 to form Fe_xO_y. The reaction was monitored using the fluorescence lifetime of pyrene as an indicator of oxygen concentration. In the absence of oxygen, pyrene has a fluorescence lifetime of ∼450 ns; however, in the presence of oxygen, the lifetime is much shorter (∼20 ns for an air-saturated solution of hexane).[13] The shorter lifetime is due to the diffusion-controlled bimolecular-

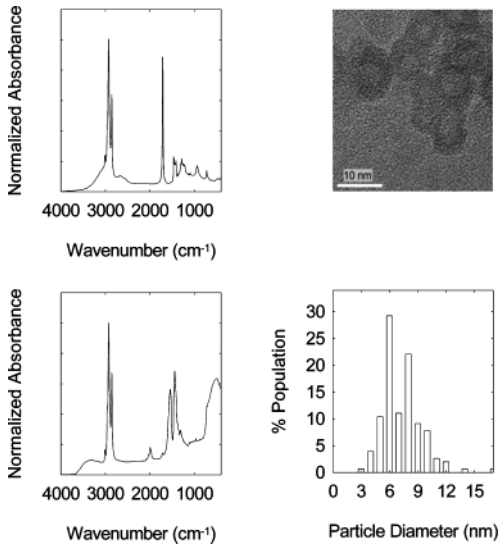

Figure 1. FTIR and TEM analyses of iron-based core−shell nanoparticles: (a) top left, FTIR neat oleic acid; (b) bottom left, FTIR iron−oleic acid nanoparticles; (c) top right, TEM of iron−AOT nanoparticles; (d) bottom right, size-distribution analysis of iron−AOT nanoparticles.

quenching reaction that occurs between pyrene and oxygen in solution. The reaction is known to follow Stern−Volmer kinetics and can therefore be used to determine the oxygen concentration quantitatively.

To obtain the baseline no-oxygen analysis, a hexane solution of pyrene was exposed to dried Fe^0 nanoparticles in a sealed reaction flask for ∼5 min with agitation. An aliquot (2.5 mL) of this solution was then transferred to a high-temperature, high-pressure stainless steel optical cell (7 mL volume) and sealed under N_2. The fluorescence decay of pyrene was then recorded using a home-assembled time-resolved fluorescence spectrometer consisting of a N_2 laser (LSI VSL-337ND), narrow band-pass filters for wavelength selection (Andover Corp., Salem, NH), and a fast-wired R928 photomultiplier tube as the detector. The instrument response function was ∼2 ns. All decays were single exponential and sufficiently long to be characterized by a linear fit of the data. The fluorescence lifetimes of pyrene in the absence of oxygen are plotted in Figure 2 as a function of temperature. At room temperature, the pyrene lifetime was measured to be 430 ns, which is in excellent agreement with previously determined values.[13] As the temperature is increased, the lifetime is observed to decrease in a systematic fashion.

To study the behavior of the core−shell nanoparticles, 2.5 mL of a 0.1 mg/mL solution of the nanoparticles in hexane (air saturated and containing pyrene) was transferred to the optical cell. The headspace was purged with N_2 to limit the initial oxygen concentration to that present in solution (∼2.7×10^{-3} M). At room temperature, the lifetime of pyrene is short (∼50 ns), indicating

10.1021/ja0473891 CCC: $27.50

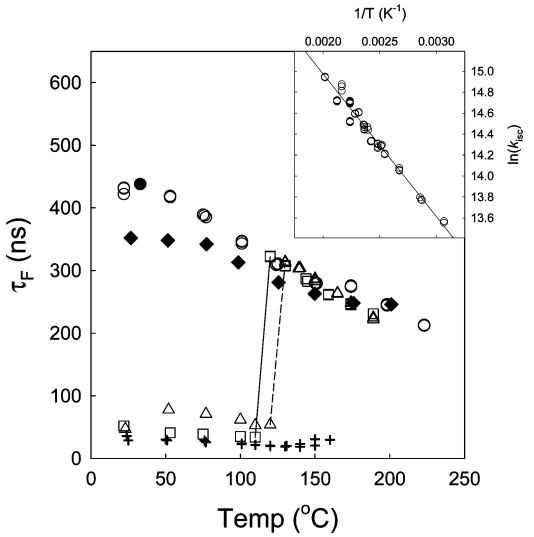

Figure 2. Plot of pyrene lifetime vs temperature for Fe^0 nanoparticles (○), iron−oleic acid nanoparticles (measured as a function of increasing temperature □ and decreasing temperature ◆), iron−AOT nanoparticles (△), and for no nanoparticles (solutions with and without oleic acid, +). Inset: Arrhenius plot of ln(k_{isc}) vs temperature.

the presence of oxygen in solution. The oxygen concentration determined from this lifetime using the Stern−Volmer equation and a diffusion rate constant of 1.7×10^{10} $M^{-1}s^{-1}$ for hexane was $\sim 1 \times 10^{-3}$ M, which was lower than the initial concentration because of partitioning between the solution and the headspace within the cell. The lifetime of pyrene remained short for temperatures up to ~110 °C, above which it increased to match the baseline-study values exactly (Figure 2). The change in lifetime is abrupt, occurring over a 10 °C temperature range, and reproducible. Pyrene decays were also recorded from high to low temperature (Figure 2). The lifetimes determined while reducing the temperature remained long, but slightly shorter than those obtained in the absence of oxygen, indicating for the most part an irreversible reaction.

For comparison, pyrene decays were also obtained in air-saturated hexane (both with and without oleic acid) without the Fe nanoparticles. Under these conditions, the lifetime of pyrene is short and remains short throughout the temperature range investigated (Figure 2).

For pyrene it is known that the decay of the first excited singlet state S_1* occurs through two routes, fluorescence (k_F) and intersystem crossing (k_{isc}), and that the sum of the quantum efficiencies of these two processes (Φ_F and Φ_{isc}) is unity.[13,14] Under these conditions, the temperature dependence of the fluorescence lifetime is attributed to intersystem crossing, and the dependence of k_{isc} on temperature follows Arrhenius kinetics.[15−18] A plot of ln(k_{isc}) vs $1/T$ (K) using all of the oxygen-free data from Figure 2 is linear, which suggests that no other processes are competing with intersystem crossing, and yields an energy barrier of 2.7 kcal/mol (Figure 2, inset). This value is somewhat smaller than previously determined values for pyrene[13] but is in good agreement with the values obtained from studies of the temperature dependence of k_{isc} for other polyaromatic hydrocarbons.[13−15]

The results of these experiments indicate that the long lifetimes obtained for pyrene at temperatures above ~110 °C are indeed due to the removal of oxygen from the optical cell. The fact that the lifetime of pyrene remains short in the absence of the Fe nanoparticles indicates the importance of Fe in this process. The intriguing aspect of these results is the ability of the core−shell nanoparticles to inhibit the oxidation of the iron core at low temperatures and then to apparently open or release over a very narrow temperature range, giving oxygen access to the iron core. Such capability suggests applications with a view toward the development of temperature-activated catalysts and reactive media. Future efforts will be focused on understanding the activation process—specifically, how molecules gain access to the core particle, whether size restrictions apply, and whether the temperature of activation can be tuned—and the nature of the reaction between oxygen and the Fe nanoparticles.

Acknowledgment. We thank Drs. J. R. Gord, D. K. Phelps, E. A. Guliants, and S. W. Buckner for helpful discussions, P. Pathak and Prof. Y.-P. Sun for TEM assistance, N. L. Sanders for experimental assistance, and Ms. M. M. Whitaker for editorial support. We acknowledge the continuing support of Dr. Julian Tishkoff and the Air Force Office of Scientific Research (AFOSR) for high-temperature fluids research.

References

(1) Caruso, F. *Adv. Mater*. **2001**, *13*, 11−22.
(2) Zhong, C.-J.; Maye, M. M. *Adv. Mater*. **2001**, *13*, 1507−1511.
(3) Crooks, R. M.; Zhao, M.; Sun, L.; Chechik, V.; Yeung, L. K. *Acc. Chem. Res*. **2001**, *34*, 181−190.
(4) Templeton, A. C.; Wuelfing, W. P.; Murray, R. W. *Acc. Chem. Res*. **2000**, *33*, 27−36.
(5) Suslick, K. S.; Fang, M.; Hyeon, T. *J. Am. Chem. Soc*. **1996**, *118*, 11960−11961.
(6) Suslick, K. S.; Hyeon, T.; Fang, M. *Chem. Mater*. **1996**, *8*, 2172−2179.
(7) (a) Shafi, K. V. P. M.; Ulman, A.; Yan, X.; Yang, N.-L.; Estournès, C.; White, H.; Rafailovich M. *Langmuir* **2001**, *17*, 5093−5097. (b) Wu, N.; Fu, L.; Su, M.; Aslam, M.; Wong, K. C.; Dravid, V. P. *Nano Lett.* **2004**, *4*, 383−386.
(8) Kataby, G.; Cojocaru, M.; Prozorov, R.; Gedanken, A. *Langmuir* **1999**, *15*, 1703−1708.
(9) Sun, S.; Murray, C. B. *J. Appl. Phys*. **1999**, *85*, 4325−4330.
(10) Puntes, V. F.; Krishnan, K. M.; Alivisatos, P. *Appl. Phys. Lett*. **2001**, *78*, 2187−2189.
(11) Sun, S.; Murray, C. B.; Weller, D.; Folks, L.; Moser, A. *Science* **2000**, *287*, 1989−1992.
(12) Mizukoshi, Y.; Fujimoto, T.; Nagata, Y.; Oshima, R.; Maeda, Y. *J. Phys. Chem. B* **2000**, *104*, 6028−6032.
(13) Birks, J. B. *Photophysics of Aromatic Molecules*; Wiley-Interscience: London, 1970.
(14) Klessinger, M.; Michl, J. *Excited States and Photochemistry of Organic Molecules*; VCH: New York, 1995.
(15) Hirano, H.; Azumi, T. *Chem. Phys. Lett.* **1982**, *90*, 269−271.
(16) Lim, E. C.; Laposa, J. D.; Yu, J. M. H. *J. Mol. Spectrosc*. **1966**, *19*, 412−420.
(17) Tanaka, F.; Okamoto, M.; Hirayama, S. *J. Phys. Chem*. **1995**, *99*, 525−530.
(18) Dreeskamp, H.; Pabst, J. *Chem. Phys. Lett*. **1979**, *61*, 262−265.

JA0473891